INVERSION OF SYNTHETIC APERTURE RADAR INTERFEROGRAMS FOR SOURCES OF PRODUCTION-RELATED SUBSIDENCE AT THE DIXIE VALLEY GEOTHERMAL FIELD

Bill Foxall

Lawrence Livermore National Laboratory
L-203, P.O. Box 808
Livermore, CA 94551
e-mail: bfoxall@llnl.gov

Don Vasco

Earth Science Division, Building 90
Lawrence Berkeley National Laboratory
1 Cyclotron Road
Berkeley, CA 94720
e-mail: dwvasco@lbl.gov

ABSTRACT

We used synthetic aperture radar interferograms to image ground subsidence that occurred over the Dixie Valley geothermal field during different time intervals between 1992 and 1997. Linear elastic inversion of the subsidence that occurred between April, 1996 and March, 1997 revealed that the dominant sources of deformation during this time period were large changes in fluid volumes at shallow depths within the valley fill above the reservoir. The distributions of subsidence and subsurface volume change support a model in which reduction in pressure and volume of hot water discharging into the valley fill from localized upflow along the Stillwater range frontal fault is caused by drawdown within the upflow zone resulting from geothermal production. Our results also suggest that an additional source of fluid volume reduction in the shallow valley fill might be similar drawdown within piedmont fault zones. Shallow groundwater flow in the vicinity of the field appears to be controlled on the NW by a mapped fault and to the SW by a lineament of as yet unknown origin.

INTRODUCTION

Ground surface deformation has been monitored at several geothermal fields employing leveling and GPS (e.g. Mossop and Segall, 1999, Vasco et al., 2002), and, more recently, synthetic aperture radar (SAR) interferometry (InSAR) using data from satellite-borne sensors (e.g. Massonet et al., 1997; Carnac et al., 1999; Fialko and Simons, 2000; Vasco et al, 2001). The sub-centimeter measurement accuracy and high (~10 m) spatial resolution afforded by InSAR can provide strong constraints on the subsurface fluid volume changes that are the sources of surface deformation above producing geothermal fields. Such volume changes are the response to fluid flow and pressure changes within the reservoir and its surroundings resulting from production activities. The surface displacements can be inverted for the time-dependent distribution of fluid volume, which potentially provides information about the geological and permeability structures of the reservoir. Indirect responses to production in the form of changes in fluid flow in the shallow subsurface above the reservoir can generate localized surface displacements. While these can be large enough to mask the direct response to production, they can potentially still provide insights into the structure and fluid regime useful, for example, in interpreting shallow temperature gradient data for planning field development (e.g Blackwell et al., 2000).

Subsidence over the Dixie Valley geothermal field has been manifest since 1996 in the form of a small subsidence bowl at the toe of the Senator alluvial fan and ground cracking that extends on to the fan itself (Allis et al., 1999). The subsidence accompanied the appearance of a line of steam vents on the fan extending SE from the pre-existing (i.e. pre-production) Senator fumarole to the toe of the fan. Allis et al. (1999) ascribe the source of this localized subsidence to reduction in pore fluid pressure in aquifers composed of permeable fan material (alluvium and landslide debris), and resulting compaction of poorly consolidated lake deposits interfingered with the fan material at the toe of the fan. According to this model, hot water flowing up the main bounding fault of the Stillwater range within a localized zone beneath the Senator fumarole

discharges laterally into the valley along permeable zones in the lower fan. Drawdown at production depths (2.5-3 km) since development began has reduced the fluid pressure in the upflow and outflow zones on the order of 10 bars in the 50-300 m depth range, which as a result is now steam dominated. The pressure reduction in the main outflow zone, identified as an aquifer 10 m below the valley floor, is estimated to be less than 2 bars. Some of the formerly liquid hot water outflow in this layer now escapes to the surface as steam.

We processed European Space Agency ERS-1 and ERS-2 satellite C-band SAR data to produce interferograms which image surface deformation that occurred in the Dixie Valley region over several intervals during the 1992-1997 time period. The interferograms image the full extent of subsidence over the Dixie Valley field. Linear elastic inversion of the subsidence map derived from the interferogram covering a 10.5-month interval between 1996-1997 confirmed that the dominant sources of deformation during this time period were large changes in fluid volumes above the reservoir itself. The detailed distributions of subsidence and volume changes support the drawdown model of Allis et al. (1999) as a likely mechanism responsible for the localized large changes in fluid volume in the vicinity of the Senator fan. The data and inversion results southwest of the Senator fan suggest that an additional source of fluid volume reduction in the shallow valley fill might be drawdown within piedmont fault zones resulting from production from the Section 33 and Section 7 wellfields.

DATA ANALYSIS

Synthetic Aperture Radar Data Processing

Table 1 summarizes the interferograms we constructed from five ERS-1/2 SAR scenes centered on Dixie Valley.

Table 1. *Orbit pairs for ERS-1/2 descending Track 213, Frame 2804*

Orbit 1	Orbit 2	Time Interval	ΔT	B_{perp} (m)
2-10087	2-12091	3/35/97 - 8/12/97	4.8 mo	3
2-5077	2-10087	4/09/96 - 3/25/97	10.5 mo	5
2-5077	2-12091	4/09/96 - 8/12/97	1.3 yr	8
1-5869	1-24750	8/29/92 - 4/08/96	3.5 yr	11
1-5869	2-10087	8/29/92 - 3/25/97	4.5 yr	93

The reader is referred to the review article by Burgmann et al. (2000) for details of the InSAR method and processing sequence. The radar phase differences mapped in the interferograms are proportional to the difference between the two orbits in the slant path lengths (ranges) from the radar to each resolution element (pixel) on the ground. These range changes include a contribution from topography in addition to displacements of the ground surface that occur in the time interval between the orbits. Therefore, in general the topographic contribution has to be removed to recover the displacement contribution. However, the sensitivity to topography is proportional to the distance between the orbit positions (B_{perp} in Table 1). The very short baselines of the first four orbit pairs in Table 1 mean that the interferograms are virtually insensitive to topography and are therefore ideal for displacement mapping over the rugged Basin and Range topography. The phase differences are converted to range changes by unwrapping the interferogram (Burgmann et al., 2000). All three components of ground displacement are projected on to the range change vector in the slant range direction and cannot be resolved from the InSAR data alone. In general, displacements related to geothermal production activities are expected to be predominantly vertical, in which case positive range change corresponds to subsidence.

We selected the 10.5-month (orbits 5077-10087) interferogram for detailed analysis. This interferogram covers the 1996-1997 period, when effects related to subsidence were first noticed at the Dixie Valley field and steam vents first appeared SE of the Senator fumarole. This orbit pair spanned sufficient time for significant surface deformation to accumulate over the Dixie Valley field, and yet preserved good phase coherence (Burgmann et., 2000) over much of the image.

Subsidence Map

Figure 1 shows the range change map in the vicinity of the Dixie Valley field. The range changes are superimposed on the radar backscatter intensity, which images the topography. The trace of the main range front fault is located at the range/valley contact indicated on the figure. Figure 1 also shows the surface fault traces within the valley interpreted by Smith et al. (2001), and the locations of the Senator fumarole and geothermal production (Sections 7 and 33) and injection (Sections 5 and 18) wells.
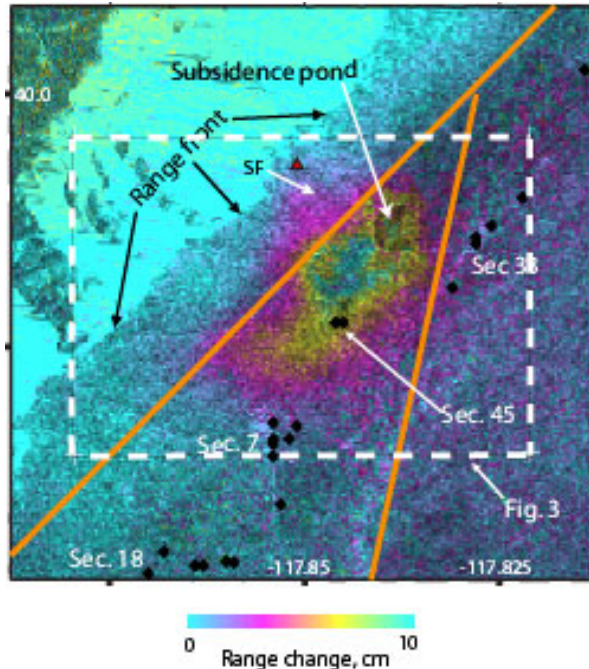
Figure 1. Map of range change over the Dixie Valley field, 4/96-3/97. Faults mapped by Smith et al. (2001) shown in orange. Red triangle shows the location of the Senator fumarole, black circles geothermal production and injection wells. SF – Senator fan.

Subsidence over the Dixie Valley field is centered slightly to the NE of the Section 5 injection wells and trends NE-SW parallel to the range front. The Section 33 and Section 7 production areas are both located outside of the area of significant subsidence. The zone of most rapid subsidence is centered about 1.2 km SE of the Senator fumarole at the toe of the Senator fan, and reaches a maximum of approximately 10 cm, a rate of about 10.5 cm/yr. This zone is immediately SW of the subsidence bowl visible on the ground. However, the bowl was filled with water at the time (3/97) of the second orbit resulting in localized phase decorrelation (Burgmann et al., 2000). Therefore, the interferogram does not image the true displacement over the bowl and the zone of most rapid subsidence probably extends further NE to incorporate it.

The 4.8-month (3/97-8/97) interferogram clearly images the same pattern of subsidence as shown in Figure 1. A similar pattern is also distinctly discernable in the 3.5-year interferogram covering the 8/92-4/96 time period, although in this case the interferogram suffers from significant phase decorrelation.

Inversion

We inverted the range change map for subsurface fractional volume change sources using the linear elastic inversion methodology described by Vasco et al. (2000, 2001). Fractional volume changes are computed within grids of rectangular source cells occupying different depth layers. The relationship between fractional volume change in the subsurface and range change is linear (Vasco et al. 2001), so that each range change estimate in the InSAR image provides a linear data constraint on volume change in the subsurface. Within the dashed box in Figure 1 some 31,104 range change observations constrain the volume change model. We solved the penalized least squares problem using an iterative algorithm. Because of the nature of surface deformation observations, depth resolution of subsurface volume changes is limited, which leads to inherent non-uniqueness in the distribution of volume change as a function of depth. To address this, the constraints provided by the data are augmented by regularization terms that bias the model towards a smoothly varying minimum magnitude solution (Vasco et al. 2001). The regularization comprises model norm and both lateral and depth roughness penalty terms. The relative weighting of the norm and roughness penalties is determined by trial and error during a series of inversions in which the penalty weights are varied. The fit to the range change observations and the model roughness are examined after each inversion with the goal of constructing a relatively smooth model that fits the observations within their estimated errors.

In order to explore the range of possible models we constructed two types of volume change models.

Three-layer inversion

The first model consisted of three horizontal layers extending from the surface to a depth of three kilometers. Each layer is one kilometer thick and is sub-divided into a grid of 41 by 41 rectangular cells, each of which can undergo a distinct volume change. This three-layer model is exploratory in nature, allowing volume changes throughout the depth range between the surface and the main production zone at 2.5-3 km depth. In order to explore the possible depth distribution of subsurface volume change we shifted the entire model down and examined the squared misfit to the data as a function of depth to the top of the model. Figure 2 shows that significant volume change is required above a depth of 1 km to yield an acceptable fit to the observations.
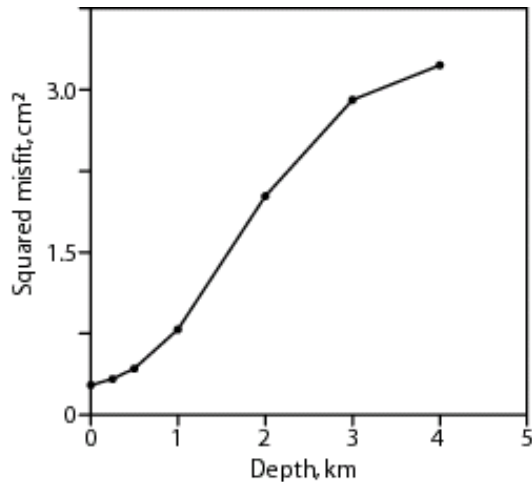
Figure 2. Squared misfit to the data versus depth to the top of the three-layer model

The best-fitting volume change distributions in the three layers are shown in Figure 3. The short wavelength variations in the high amplitude range change observations require that most of the volume change be confined to the uppermost (0-1 km) layer. The inversion also produced substantial apparent volume change in the bottom two layers. However, the patterns of volume changes in these layers essentially mimic the distribution in the upper layer, the most prominent features of which are closely correlated with localized features on the ground surface (see below). This suggests that the solutions in the lower layers are largely dominated by smearing of the short wavelength volume changes in the upper layer due to the degrading resolution of the data with increasing depth.

Shallow inversion

Given the apparent dominance of short wavelength volume change sources in the shallow subsurface, the second model consisted of a single shallow, horizontal layer extending from 100 meters to 500 meters in depth, and divided into a grid of 41 by 41 rectangular cells. This layer corresponds to valley fill above faulted basement within about 2 km of the range front (e.g. Blackwell et al., 1999). The inversion procedure was the same as that for the three-layer model except that no depth smoothing was employed. As before, the regularization weighting was determined by trial and error.

The results for the single layer model are shown in Figure 4. The pattern of volume changes is similar to that in the upper layer of the three-layer model, but more localized. Restricting the source layer to be 400 m thick results in large localized fractional volume changes as high as 4×10^{-2}.
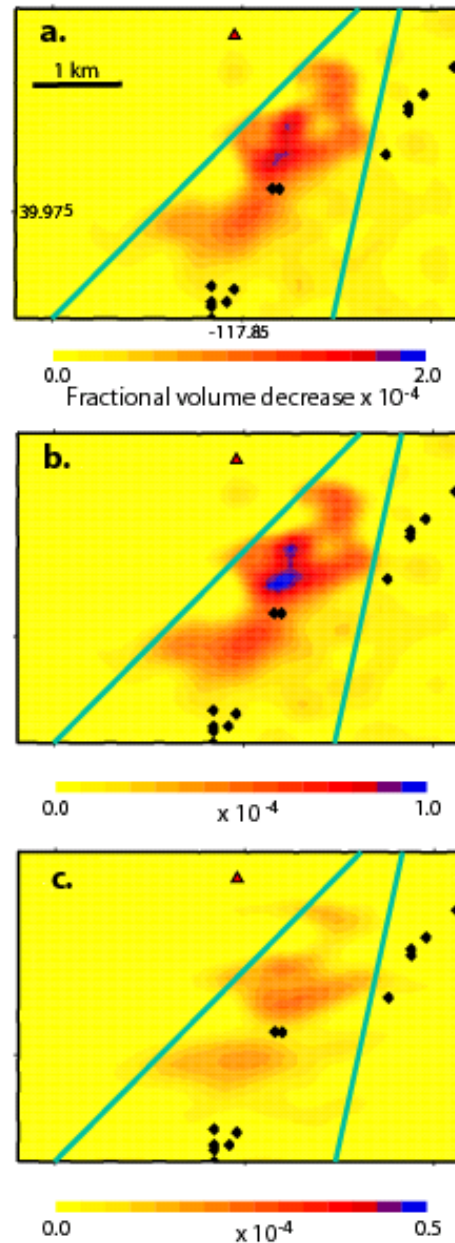

*Figure 3. Fractional volume reduction in the three-layer inversion model: (**a**) 0-1 km; (**b**) 1-2 km; (**c**) 2-3 km. Note different color scale for each layer. See Fig. 1 for explanation of symbols.*

DISCUSSION

The inversion results indicate that the short spatial wavelength of the high amplitude subsidence pattern over the Dixie Valley field requires that the predominant volume change sources must be shallow, and probably confined to the valley fill. The

single layer inversion indicates very high (~10^{-2}/yr) fractional volume reduction rates in a localized shallow zone at the toe of the Senator fan and in the valley fill immediately adjacent to the south (and most likely also to the north). Southwest of this zone the northwestern edge of the subsidence area is almost coincident with the trace of the valley fault mapped by Smith et al. (2001) (Figure 1), but then it deviates to the NW to encompass the Senator fan and the hot outflow plume (Allis et al., 1999; Blackwell et al., 2000). Subsidence terminates on the NW in the vicinity of the Senator fumarole. Subsidence rates over the fan were in the range 1-3 cm/yr.
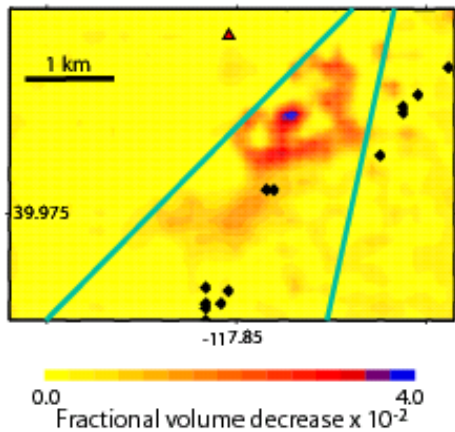

Figure 4. Fractional volume reduction in the single shallow layer inversion model. See Fig. 1 for explanation of symbols.

The close conformance of the subsidence pattern with the Senator fan and fumarole, and the location of the zone of most rapid volume reduction at the toe of the fan lend support to the fluid pressure decline model of Allis et al. (1999) as a likely mechanism responsible for the most rapid subsidence. The single layer inversion solution suggests that the zone of relatively lower rate volume reduction in the southwestern part of the model is connected with the zone adjacent to the fan. According to the Allis et al. model, this would indicate that the outflow affected groundwater flow almost as far south as the northernmost Section 7 well. The southern boundary of the outflow plume defined by shallow temperature gradients is located roughly half way between the Senator fan and the Section 7 wells (Allis et al., 1999, Fig. 5), and the shallow temperature gradients in the Section 7 wells are close to the valley background. This suggests that groundwater under the southwestern end of the subsidence area is in equilibrium with cold valley aquifers and that relatively small reductions in fluid pressure results from northeasterly flow towards the low-pressure zone at the toe of the Senator fan.

The near coincidence of the northwestern edge of the subsidence with the mapped fault trace SW of the fan suggests that shallow groundwater flow is confined SE of the fault. This is also suggested by the shallow inversion solution in Figure 4. The eastern edge of the subsidence is more diffuse but roughly coincides with a NNE-striking surface fault mapped by Smith et al. (2001) (Figure 1), which might act as a barrier to flow to the east. However, the eastern boundary of shallow volume change in Figure 4 matches rather well the eastern limit of a transparent zone in seismic reflection data (e.g. Smith et al., 2001, Fig. 1), which may correspond to relatively permeable alluvium/landslide debris or fractured basement rock.

The southwestern edge of the subsidence is remarkably linear. This boundary is closely aligned with a prominent ENE-WNW-trending lineament that is distinct at least as far as the center of the valley about 4 km east of the geothermal field on both the SAR backscatter intensity image and interferogram, and on Landsat. Although the alignment might be fortuitous, it suggests transverse structural control of groundwater flowing parallel to the valley, in this case by a regional-scale feature. We are continuing to investigate the nature of this lineament and the possible role that the causative structure might play in the valley groundwater regime and in localizing the geothermal resource at Dixie Valley. However, this structure, if it exists, evidently does not affect flow within the production zone as connectivity between the Section 5 injectors and Section 7 producers was demonstrated by Rose et al. (1997).

Recent work (e.g. Blackwell et al., 1999) indicates that the Dixie Valley production zone includes steeply dipping piedmont faults in addition to the main range-bounding fault. Blackwell et al. (2000) point out that if this is the case, then the Section 33 and 7 production zones cannot be located on the range bounding fault, the source of outflow at the Senator fumarole, but must be on a piedmont fault or faults. The exact locations and subsurface geometries of candidate faults have yet to be determined. A schematic cross-section by Blackwell et al. (1999, Fig. 6) (also Blackwell, unpublished) shows a blind piedmont fault that offsets basement against valley fill as shallow as 300-500 m under the valley. Such faults may continue to shallow depths within the valley fill or might reach the valley floor, perhaps along the traces mapped by Smith et al. (2001). Blackwell et al. (2000) argue that upflow on the piedmont faults would discharge into the valley fill, if it occurred naturally prior to production. Therefore, a possible alternative explanation for the modest subsidence and volume reduction south of the Senator fan is decrease in the pressure of fluid outflow into relatively deep aquifers due to drawdown on piedmont faults. East of the Senator fan the subsidence related to reduction in shallow

outflow from the range front would be superimposed on this lower amplitude signal. A third potential source of subsidence we are presently investigating is reduction of fluid volume at and above production depths within a dipping piedmont fault zone itself.

CONCLUSIONS

Synthetic aperture radar interferograms spanning several time intervals during the 1992-1997 time period image ground subsidence over the Dixie Valley geothermal field. The interferogram for a 10.5 month period between 4/96 and 3/97 images rapid subsidence locally reaching about 10.5 cm/yr over the northern part of the field, between the Section 33 and Section 7 production areas. We inverted the range change map derived from the 4/96-3/97 interferogram for the distribution of fluid volume change sources within horizontal layers between the ground surface and 3 km depth. The inversions require the dominant sources of subsidence to be located at less than 1 km depth within the valley above the production zone. Restricting the sources to the upper 500 m yielded rates of fractional volume reduction on the order of 10^{-2}/yr over the northern part of the production zone during the 1996-1997 time period.

The distributions of subsidence and volume sources in the vicinity of the Senator fan support the model proposed by Allis et al. (1999). In this model production-induced drawdown within an upflow zone localized beneath the Senator fumarole caused a large reduction in the pressure of hot water discharged into the valley fill. Lesser volume changes south of the Senator fan could be the result of groundwater flow towards the zone of lowest pressure at the toe of the fan. Alternatively, these volume changes could be caused by reduction in fluid outflow from one or more piedmont faults, which have been proposed as the sources for geothermal production in Sections 33 and 7. We are not able to discriminate between these alternatives based on our present inversion results. A third potential source of subsidence that we are presently investigating is reduction in fluid volume within piedmont fault zones themselves. Finally, our results suggest that groundwater flow within the valley is controlled by longitudinal and transverse geological structures identified on the surface.

REFERENCES

Allis, R.G., S.D. Johnson, G.D. Nash, D. Benoit (1999), "A model for the shallow thermal regime at Dixie Valley geothermal field, *Geothermal Resources Council Trans.*, **23**, 493-498.

Burgmann, R., P.A. Rosen, and E.J. Fielding (2000), "Synthetic aperture radar interferometry to measure Earth's surface topography and its deformation", *Ann. Rev. Earth & Planetary Sci.*, **28**, 169-209.

Blackwell, D.D., K.W. Wisian, D. Benoit, and Bobbie Gollan (1999), "Structure of the Dixie Valley geothermal system, a "typical" basin and range geothermal system, from thermal and gravity data", *Geothermal Resources Council Trans.*, **23**, 525-531.

Blackwell, D.D., B. Golan, and D. Benoit (2000), "Temperatures in the Dixie Valley, Nevada geothermal system", *Geothermal Resources Council Trans.*, **24**, 24-27.

Carnac, C, and F. Hubert (1999), "Monitoring and modeling land subsidence at the Cerro Prieto geothermal field, Baja California, Mexico, using SAR interferometry", *Geophys. Res. Lets*, **26**, 1211-1214.

Fialko, Y, and M. Simons (2000), "Deformation and seismicity in the Coso geothermal area, Inyo County, California; observations and modeling using satellite radar interferometry", *Jo. Geophys. Res.*, **105**, 21,781-21,793.

Massonnet, D., T. Holzer, and H. Vadon (1997), "Land subsidence caused by the East Mesa geothermal field, California, observed using SAR interferometry ", *Geophys. Res. Lets.*, **24**, 901-904.

Mossop, A., and P. Segall (1999), "Volume strain within the Geysers geothermal field", *Jo. Geophys. Res.*, **104**, 29,113-29,131.

Rose, P.E., K.D. Apperson, S.D. Johnson, and M.C. Adams (1997), "Numerical simulation of a tracer test at Dixie Valley, Nevada", *Proc. 22nd Workshop on Geothermal Reservoir Eng.*, Stanford Univ., Calif., Jan. 27-29, 1997, 169-176.

Smith, R.P., K.W. Wisian, and D.D. Blackwell (2001), "Geological and geophysical evidence for intra-basin and footwall faulting at Dixie Valley, Nevada", *Geothermal Resources Council Trans.*, **25**, 323-326.

Vasco, D.W., K. Karasaki, and C. Doughty (2000), "Using surface deformation to image reservoir dynamics", *Geophysics*, **65**, 132-147.

Vasco, D.W., C. Wicks, K. Karasaki, and O. Marques (2001), "Geodetic imaging: Reservoir monitoring using satellite interferometry", *Geophys. Jo. Internat.*, **200**, 1-12.

Vasco, D.W., K. Karasaki, and O. Nakagome (2002), "Monitoring production using surface deformation: the Hijiori test site and the Okuaizu geothermal field, Japan", *Geothermics*, **31**, 303-342.